phys. stat. sol. (b) **209**, 109 (1998)

Subject classification: 72.10.Di; 71.38.+i; 72.20.Dp

Numerical Studies of the Markovian Limit of the Quantum Kinetics with Phonon Scattering

M. NEDJALKOV (a), I. DIMOV (a), and H. HAUG (b)

(a) CLPP, Bulgarian Academy of Sciences, Sofia, Bulgaria

(b) Institut für Theoretische Physik, Universität Frankfurt am Main, Germany

(Received January 16, 1998; in revised form May 15, 1998)

The contribution of the Markovian component of a quantum-kinetic model to the carrier dynamics in photoexcited semiconductors is studied for intermediate evolution times. It is shown that for zero lattice temperature two unphysical effects arise due to an exponential damping in the memory kernel, which results in the long-time limit in a Lorentz broadened energy delta function. A finite carrier density is observed in the semiclassically forbidden energy region. Also the carriers with energy below the LO phonon threshold are in mutual exchange, having a nonvanishing total out-scattering rate. It is shown that in the inverse hyperbolic cosine damping model, which corrects the Lorentzian to an inverse hyperbolic cosine, such effects are suppressed. The results provided by the two models are obtained by a Monte Carlo algorithm based on the iteration approach and allowing one-dimensional simulation.

1. Introduction

The kinetics of a system of carriers, excited by a laser pulse in a semiconductor involves processes within the femtosecond time scale and hence requires a quantum description. Several approaches can be followed. One can use the Green's functions formalism or, alternatively, one can work in terms of density matrices. If one expresses the Hamiltonian in second quantization, the physical observables are expressed as statistical averages of combinations of single particle creation and annihilation operators. Due to the interaction part of the Hamiltonian, the equations of motion of the density matrix elements as a rule introduce averages of higher number single particle operators, thus leading to an infinite hierarchy of coupled equations. In order to obtain a closed equations set, the hierarchy has to be cut to some level by appropriate approximations. Depending on the cut level and the chosen set of physical variables, a variety of quantum processes can be taken into account. If the electrons and holes distribution functions and the polarization are chosen as relevant variables, then in the free carrier description (all interactions but with the photon field neglected) the set of coherent optical Bloch equations is obtained. These equations allow to describe effects which can be observed by time-resolved spectroscopy, like Rabi flopping, photon echo, and quantum beats [1]. The equations placed deeper in the hierarchy involve a number of interaction processes. In the model proposed in [2] the set is closed by approximations in the equations of motion for different types of four operators statistical averages. The obtained semiconductor Bloch equations include together with the carrier–phonon and carrier–carrier interactions, also interference effects between different types of interactions. An example is the polarization scattering, which accounts for electron–phonon and hole–phonon interacting simultaneously.

For dilute systems the carrier–phonon interaction dominates the carrier–carrier interaction. In the low-density regime the self-energy corrections of the particle energies are very small compared to their kinetic energy. In this regime the carrier subsystem is treated as noninteracting and the carrier–phonon kinetics is explored.

The carrier–phonon kinetics beyond the semiclassical Boltzmann equation (BE) has been investigated for many years for the case of applied electrical field. In 1969 Levinson [3] derived an equation which introduces the intra-collisional field effect (ICFE), accounting for the action of the electric field during the scattering process. It broadens the energy-conserving delta function to a finite width proportional to the square root of the applied field [4]. The Levinson equation was generalized by Barker [5] for a degenerate electron gas. In [6] a model accounting for collisional broadening (CB) and ICFE was proposed and the long-evolution-time kinetics was investigated.

During the last decade the carrier–phonon quantum kinetics has been investigated for optically generated carriers [7,8]. A recent contribution is given in [2]. The relevant observables are the electron and phonon distribution functions. Their equations of motion couple to the equation for the statistical average of two electron and one phonon operators, called phonon-assisted density matrix. The set of three equations accounts for the main terms responsible for the electron–phonon scattering in the semiconductor Bloch equations. The finite lifetime of the free carriers appears as an exponential damping factor.

The set can be reduced by further approximations to an equation, which generalizes the BE. Its quantum character reveals through the memory character of the scattering process due to the time-dependent kernel and the CB due to the finite electron states lifetime. The only effect of the photon field is to introduce a time source thus allowing to cut the infinite past of the non-Markovian evolution. The source can be a term accounting for the generation of carriers, or an initial condition.

The properties of the solution can in general be investigated only numerically. The choice of an initial condition although being not the best approach from physical point of view, allows both, to ensure that the effects are numerically accessible and to study conveniently the effects of their variation. In this way the following quantum effect has been demonstrated: at short evolution times carriers can populate very high energy regions [2] due to the short-time peculiarities of the kernel. Another effect appears for large evolution times [9]. It is due to the fact that the long-time (Markovian) limit of the kernel is broadened with respect to the exact energy conservation of the semiclassical scattering process. This leads to an increasing population of high-energy states in the solutions of the time-dependent kinetic equation, called the run-away effect. The same property is exhibited by the high-field time-independent model solution [6] compared to the quasiequilibrium distribution (a heated Maxwellian).

The reason for such unphysical behaviour is in the set of approximations used to obtain the corresponding model. They are valid on the quantum scale and an extrapolation towards classical kinetics requires corresponding corrections. Recently an inverse hyperbolic cosine model, which connects the short and long times in the kinetics has been proposed in Ref. [9]. The model improves the long-time kinetics towards the equilibrium distribution considerably.

It has been shown [10] that the kernel of the integral form of the one-band quantum kinetic equation is expressed as a sum of a Lorentzian (the Markovian limit of the

kernel) and an exponentially damped, oscillating time-dependent part. For zero evolution time both components compensate each other, while for large times the Markovian limit of the kernel determines the steady state solution. Here we are interested in intermediate times, where the early-time quantum kinetics is taken in its Markovian limit and to study in detail the effects of different damping models. Since in the corresponding resolvent series only the most significant subseries are taken into account, they will approximate the exact quantum solutions. However, we can demonstrate by this approach clearly the Markovian effects introduced by the various damping. For this reason, we choose the lattice temperature to be zero and consider one optical phonon mode with a fixed energy. Then the semiclassical behaviour of the electron system obeys simple rules so that deviation from them can be clearly seen.

In the next section we consider the one-band quantum kinetics and the inverse hyperbolic cosine model. In Section 3 we present the one-dimensional Markovian form of the corresponding models, suitable for the used numerical method. It is based on the Monte Carlo iteration approach. Its algorithm, successively applied for solving the one-band quantum kinetic model, is now modified for an optimal simulation of the Markovian equations. The Monte Carlo procedure is described in the Appendix. The results and the discussion of the effects are given in Section 4.

2. The Kinetic Model

The linear three-dimensional one-band electron quantum kinetic equation has the following integral form [10]:

$$f(k,t) = \int_0^t \mathrm{d}t' \int_0^{t'} \mathrm{d}t'' \int \mathrm{d}^3q \left\{ S(k+q,k,t'-t'')\, f(k+q,t'') - S(k,k+q,t'-t'')\, f(k,t'') \right\} + \phi(k) \tag{1}$$

with

$$S(k+q,k,t-t') = \frac{2V}{(2\pi)^3 \hbar^2} \|g_q\|^2 \, \mathrm{e}^{-(\Gamma_{k+q}+\Gamma_k)(t-t')}$$
$$\times \left\{ \cos\left(\frac{\varepsilon_{k+q} - \varepsilon_k - \hbar\omega}{\hbar}(t-t')\right)(n+1) + \cos\left(\frac{\varepsilon_{k+q} - \varepsilon_k + \hbar\omega}{\hbar}(t-t')\right) n \right\}, \tag{2}$$

where n is the Bose function for equilibrium phonons, ϕ the initial condition, ε the free electron energies, ω the phonon frequency, and g the coupling constant. Here we assume Fröhlich interaction.

$$\Gamma_k = \int \mathrm{d}^3q \frac{V}{2^3\pi^2\hbar} \sum_{\pm} \|g_q\|^2 \, \delta(\varepsilon_{k+q} - \varepsilon_k \pm \hbar\omega)(n + 1/2 \pm 1/2) \tag{3}$$

is the contribution of the Boltzmann out-scattering rate giving rise to a finite lifetime of the carriers.

This equation has the same general structure as the Levinson one (taken in presence of an initial condition). The differences appear from two sources: In presence of an electric field $F(t)$, the statistical average is taken with respect to the accelerated free electron states. This results in a time dependence of k in the right-hand side of (1) according to a Newton trajectory $k(t,t') = k - \int_{t'}^{t} \mathrm{d}\tau F(\tau)/\hbar$, parametrized by k and t. This

transforms the time factor in the cosine arguments to integration in the corresponding time limits. The Levinson equation does not account for a lifetime damping factor, since the hierarchy cut is done earlier with respect to the one-band model.

Above considerations prompt that the ICFE can be also incorporated in the quantum kinetics of optically generated carriers. Also the used Monte Carlo method can be easily modified to account for the Newton trajectories.

The common way of obtaining the long-time-scale solution of a quantum kinetic equation is to use the Markov approximation. With the help of adiabatic and Markov approximations, one can obtain the BE [11]. Here we follow another approach.

Equation (1) can be processed with the help of the identity $\int_0^t \mathrm{d}t' \int_0^{t'} \mathrm{d}t'' = \int_0^t \mathrm{d}t'' \int_{t''}^t \mathrm{d}t'$ to obtain a form similar to the BE. The difference with the latter is that the "scattering kernel" depends explicitly on the time, causing memory effects in the carrier dynamics,

$$f(k,t) = \int_0^t \mathrm{d}t'' \int \mathrm{d}^3q \left[\left\{ \int_{t''}^t \mathrm{d}t' \, S(k+q,\, k,\, t'-t'') \right\} f(k+q,\, t'') - \left\{ \int_{t''}^t \mathrm{d}t' \, S(k,\, k+q,\, t'-t'') \right\} f(k,\, t'') \right] + \phi(k). \tag{4}$$

Equation (4) allows an analytical evaluation of the time integral, since

$$\int_0^{t-t''} \mathrm{d}\tau \, \mathrm{e}^{-(\Gamma_{k+q}+\Gamma_k)\tau} \cos(\Omega_{k+q,k}\tau) = \frac{(\Gamma_{k+q}+\Gamma_k)}{\Omega_{k+q,k}^2 + (\Gamma_{k+q}+\Gamma_k)^2}$$

$$\frac{-(\Gamma_{k+q}+\Gamma_k)\cos(\Omega_{k+q,k}(t-t'')) + \Omega_{k+q,k}\sin(\Omega_{k+q,k}(t-t''))}{\Omega_{k+q,k}^2 + (\Gamma_{k+q}+\Gamma_k)^2} \, \mathrm{e}^{-(\Gamma_{k+q}+\Gamma_k)(t-t'')}, \tag{5}$$

where $\Omega_{k+q,k} = (\varepsilon_{k+q} - \varepsilon_k - \hbar\omega)/\hbar$.

In this way the kernel is decomposed into a time-independent part and a part which depends explicitly on the time.

It has been proved that the resolvent series of the integral equation (4) converges [10], so that the solution can be obtained through an iteration procedure. Three subseries contribute, containing only the first part of the kernel, the second one and a mixed one, respectively. Now we can discuss qualitatively the importance of the two parts of the kernel for larger evolution times. A ready argument is that the oscillations in the time-dependent part cancel their contribution to the time integral in (4). In addition there are arguments related to the conditions of the optically generated carriers kinetics: the initial condition is a sharp function in the energy scale, placed few phonon energy steps above the energy bottom. The maximum contribution gives states around the minimum of the denominator in (5) (i.e. the exact energy conservation). If there is a well-defined direction in the choice of the after-scattering electron state ($n \ll 1$), the nonzero region of the initial condition will be encountered only within few iterations (i). Accordingly, the evolution time is divided into few intervals $t, t_1, \ldots, t_i, 0$. For small time intervals t_k, t_{k+1} the two terms in (5) have close values. But then, there exist a compensating larger time interval (since their sum equals the evolution time), where the second part of the kernel is damped effectively. Above some intermediate evolution times

t, the mean value of the subintervals t/i is such that the time-independent part of the kernel dominates due to the effect of the exponential damping. These considerations illustrate the concept of the coarse graining in time – the heuristic base of the Markovian limit in quantum kinetics.

For GaAs parameters a time factor of about 200 fs drops the oscillatory kernel component by the order of three times.

By keeping only the Markovian component, (4) appears as a Boltzmann equation with a Lorentzian replacing the energy-conserving delta function,

$$f(k,t) = \int_0^t \mathrm{d}t' \int \mathrm{d}^3k' [S(k',k)\, f(k',t') - S(k,k')\, f(k,t')] + \phi(k)\,, \tag{6}$$

where

$$S(k',k) \sim |k-k'|^2 \left\{ (n+1) \frac{(\Gamma_{k'} + \Gamma_k)}{\Omega_{k',k}^2 + (\Gamma_{k'} + \Gamma_k)^2} + (n) \frac{(\Gamma_{k'} + \Gamma_k)}{\Omega_{k,k'}^2 + (\Gamma_{k'} + \Gamma_k)^2} \right\}.$$

The delta function of the Fermi golden rule is recovered if the damping Γ is let to zero in the Lorentzian. Then eqn. (6) becomes the semiclassical Boltzmann equation.

The long-time behaviour of the solution of (6) deviates from the equilibrium distribution, which is associated with the long-reaching wings of the scattering kernel.

As already noted, the extrapolation of the quantum kinetic equation towards the semiclassical time scale needs corresponding correction. The quantum kinetic treatment in terms of nonequilibrium Green's functions [9] shows where the defects of the Boltzmann kinetics with Lorentz resonance lines originate from: The damping is not constant on a femtosecond timescale, but sets in in a delayed way. In this theory the scattering memory kernel is determined by a product of the retarded and advanced Green's functions [13]. An investigation of the time-dependent non-equilibrium Dyson equation for the retarded electron GF shows that the damping first increases in time until it saturates at later time into the usual exponent. Interpolating this asymptotic behaviour by a hyperbolic tangent and inserting this damping law into the Dyson equation one finds an analytic solution in form of an inverse hyperbolic cosine [9]. Recently it has been shown, that inverse hyperbolic cosine damping describes the numerical solutions of the Dyson equation qualitatively rather well [14]. According to this result, $\mathrm{e}^{-\Gamma(t-t')}$ is replaced with $\cosh^{-\alpha}(\omega(t-t'))$, $\alpha = \Gamma/\omega$. The alpha parameter is the well-known dimensionless Fröhlich coupling parameter. It is essentially the ratio of the polaron-self-energy and the LO-phonon energy. Thus $\alpha \ll 1$ is the weak coupling regime, $\alpha \approx 1$ is the intermediate coupling regime, and $\alpha \gg 1$ is the strong coupling regime. In our model α depends on k through Γ, eqn. (3).

This damping law shows that the coherence of the electron waves is not immediately destroyed by the collisions, but the decay starts in form of a Gauss function. In the Fourier space, the modified short-time damping has influence on the large-frequency wings of the resonance. It cuts off the trouble-causing long-ranging wings of the Lorentzian resonance. The model provides for evolution times near the equilibrium a distribution function close to the equilibrium distribution.

Here we investigate the effects carried by the Markovian parts of the two models for the intermediate evolution time region, where a build-up of the coarse grainig in time is expected.

The time-dependent solutions of eqn. (6) with the corresponding kernels are obtained by Monte Carlo simulation.

The Markovian limit of the interpolation model is given by the (0 to ∞) time integral of the kernel. A simplification is to insert α in the argument of the inverse hyperbolic cosine and to use the formula

$$\int_0^\infty \mathrm{d}t \frac{\cos(\Omega t)}{\cosh(\Gamma t)} = \frac{\pi}{2\Gamma} \cosh\left(-\frac{\pi\Omega}{2\Gamma}\right).$$

For GaAs such substitution simply makes the effects to be more pronounced, which is in correspondence with the aim of this work.

3. The One-Dimensional Equation

An isotropic initial condition reduces the dimensions of the equation to one. In spherical coordinates, with k and k' denoting the norm of the corresponding vectors, the equation is

$$f(k,t) = \int_0^t \mathrm{d}t' \int_0^K \mathrm{d}k'\, G_s \frac{k'}{k} \ln\left(\frac{k+k'}{|k-k'|}\right) \{\mathcal{K}(k', k) f(k', t') - \mathcal{K}(k, k') f(k, t')\} + \phi(k), \tag{7}$$

where $\mathcal{K}(k', k)$ is constructed either by the Lorentzian or by $\frac{\pi}{2(\Gamma(k)+\Gamma(k'))} \times \cosh\left(-\frac{\pi\Omega_{k',k}}{2(\Gamma(k)+\Gamma(k'))}\right)$. G_s is a constant. The k-dependence of Γ is

$$\Gamma(k) = \frac{g(n+1)}{k} \ln\left(\frac{\sqrt{\omega_1}}{k-\sqrt{k^2-\omega_1}}\right) + \frac{gn}{k} \ln\left(\frac{\sqrt{\omega_1}}{-k+\sqrt{k^2+\omega_1}}\right),$$

where $\omega_1 = 2m\omega/\hbar$, g is a constant and the first term is counting if $k^2 \geq \omega_1$.

Eqn. (7) cannot be treated as a one-dimensional Boltzmann equation, since there is no symmetry of the kernels with respect to the $k - k'$ exchange. In this case, the traditional Ensemble Monte Carlo must be carried out in three dimensions, i.e. equation (6) will be simulated. Here we apply the numerical Monte Carlo approach, which allows a one-dimensional simulation.

The iteration series for an equation with the structure of eqns. (1), (6), (7) contains positive and negative terms which have to cancel effectively in the numerics. This leads to a large variance of the Monte Carlo procedure [12], thus requiring massively parallel computers for evolution times of the order of hundreds femtoseconds [10]. Fortunately, the time independent kernel in the Boltzmann equation (7) allows another integral form,

$$f(k,t) = \int_0^t \mathrm{d}t' \int \mathrm{d}^3k'\, S(k', k)\, \mathrm{e}^{-\lambda(k)(t-t')} f(k', t') + \mathrm{e}^{-\lambda(k)t} \phi(k). \tag{8}$$

Here $\lambda(k) = \int \mathrm{d}^3k' S(k, k')$ is the probability per unit time for an electron to be scattered out of state k. In the semiclassical case $\lambda = \Gamma$. It enables an effective stochastic approach for large evolution times.

4. Simulation Results

For long evolution times, the quantum mechanical picture proceeds to the semiclassical one, where the Boltzmann equation provides the adequate physical description of the electron–phonon kinetics. The electron–phonon interaction then is presented by the Fermi golden rule, where the conservation law links the kinetic energies of the electron before and after the scattering event with the phonon energy. At zero temperature, as long as the hot phonon effects are excluded, the electrons can only loose their kinetic energy. It is reduced at each scattering event with a quantity equal to the energy of the interacted phonon. For the case of constant phonon energy, the evolution of the distribution function is presented by replicas of the initial distribution, shifted towards low energy. The electrons cannot be scattered out of the states below the phonon energy ($\lambda(k) = 0$ if $\varepsilon_k < \hbar\omega$) and cannot appear above the initial distribution. This simple physical behaviour of the electron system will be the reference background for the effects introduced by the two damping models.

The results discussed in the following are obtained by Monte Carlo simulation of the equations corresponding to the two damping models. Material parameters for GaAs are used: the electron effecive mass is 0.063, the optical phonon energy is 36 meV, the static and optical dielectric constants in the Fröhlich coupling are 10.92 and 12.9, respectively. The lattice temperature is zero. The initial condition is given by a Gaussian in energy, corresponding to a 87 femtosecond laser pulse with an excess energy of 180 meV, scaled in a way to ensure peak value equal to unity. The quantity presented on the y-axes in Figs. 1 to 6 is $k \cdot f(k, t)$, i.e. it is proportional to the distribution func-

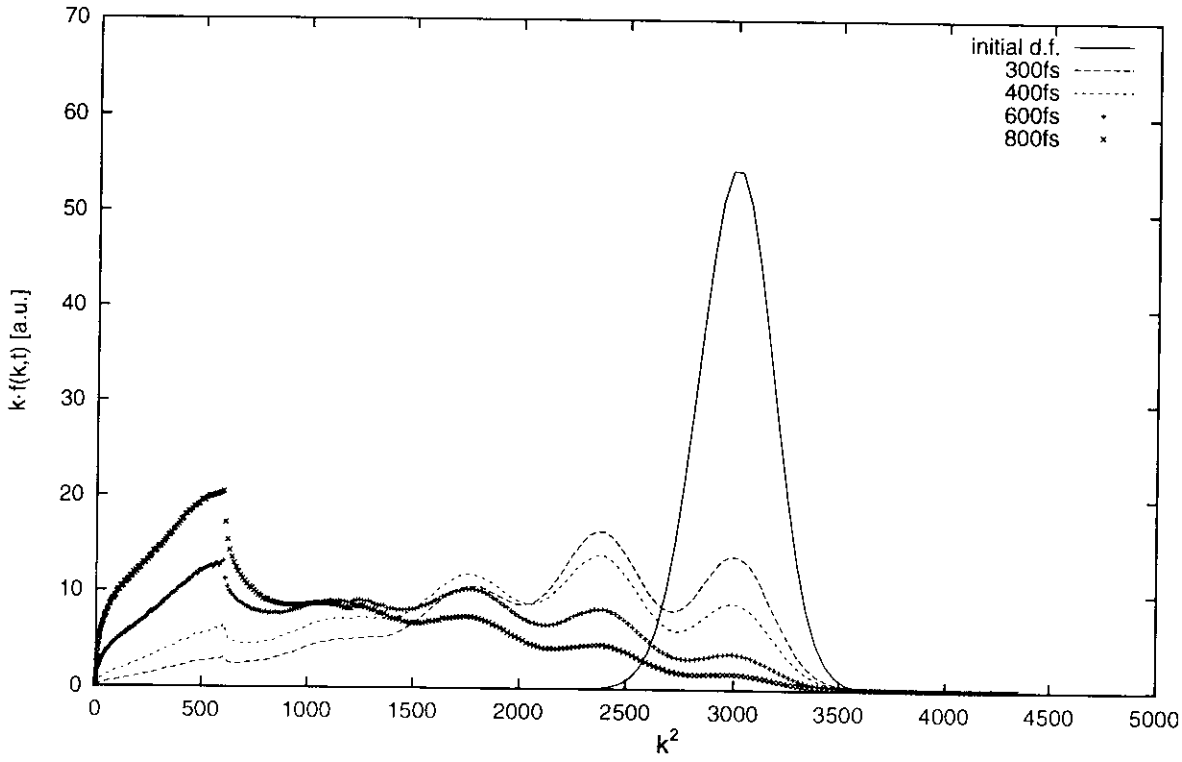

Fig. 1. The electron distribution $k \cdot f(k, t)$ versus k^2 for the Markovian model. The evolution time is 300, 400, 600, and 800 fs, respectively. The place of the phonon threshold is indicated by the discontinuity of the curves. The replica-like structure dissapears in the low-energy region

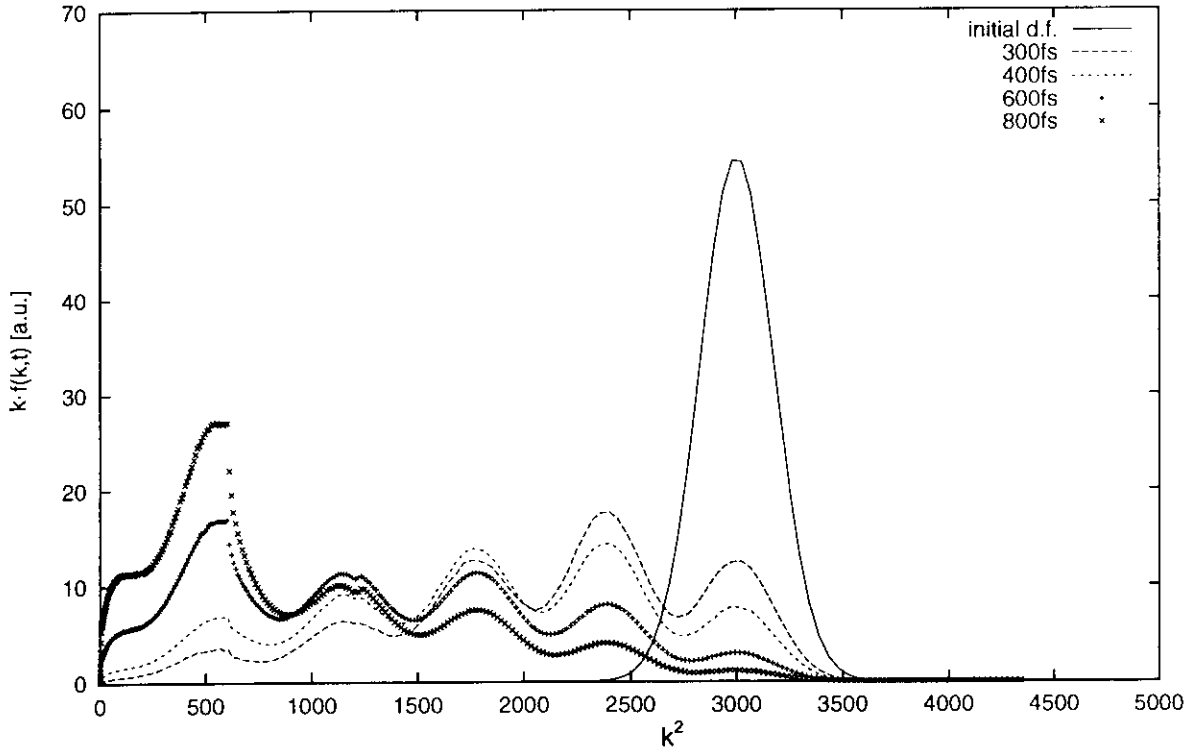

Fig. 2. The electron distribution $k \cdot f(k,t)$ versus k^2 for the inverse hyperbolic cosine model. The evolution time is 300, 400, 600, and 800 fs, respectively. The replica-like structure is well pronounced in the low-energy region

tion multiplied by the density of states, and is given in arbitrary units. The quantity k^2, given on the x-axes in units $10^{14}/\mathrm{m}^2$, is proportional to the electron energy.

In Figs. 1 and 2, the solutions of the models with exponential and inverse hyperbolic cosine damping are presented, respectively. The evolution time varies between 300 fs, when a small fraction of carriers is below the phonon threshold, and 800 fs when there are almost no electrons in the initial condition region. Above this interval the peak of the distribution function exceeds unity, so that the degeneracy of the carrier system has to be included in the models.

Because of the onset of Γ, there is a discontinuity of the kernels leading to discontinuity in the solution around the phonon threshold. The jump in the semiclassical distribution function is $\Gamma(k_t)\int_0^t f(k_t,t')\,\mathrm{d}t'$, where k_t corresponds to the phonon energy. Similarly, the jump in the solutions of the two models increases with the time.

The Lorentzian model solution looses the replica-like structure towards the energy bottom. In contrast the inverse hyperbolic cosine model keeps the pattern in the low-energy region. Its peaks are better pronounced as it is seen from the comparison of the 400 and 600 fs solutions in Figs. 3 and 4.

Fig. 5. shows the run-away effect at 10, 40, and 400 fs for the Lorentzian model. The carrier population in the semiclassically forbidden energy region increases with the time. The ratio between the distribution function values in the run-away region to the peak value in the initial condition region is of order of 10^{-3} for 10 and 40 fs, while for 400 fs it increases to 10^{-2}. For such a time, the number of electrons in the initial peak region drops by six times. The upper energy region is fed up by the electrons in the

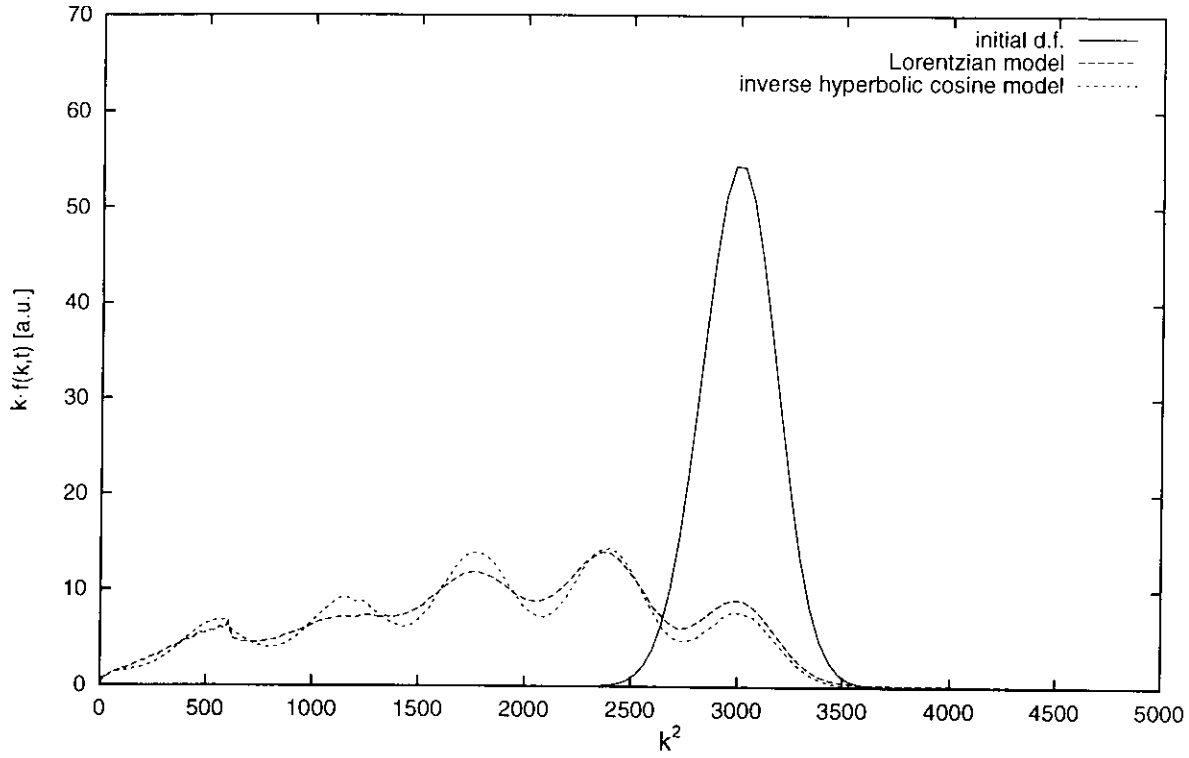

Fig. 3. Comparison of the electron distribution $k \cdot f(k,t)$ versus k^2 obtained by the two damping models for evolution time 400 fs. The replica-like structure for the inverse hyperbolic cosine model is extended in the whole interval

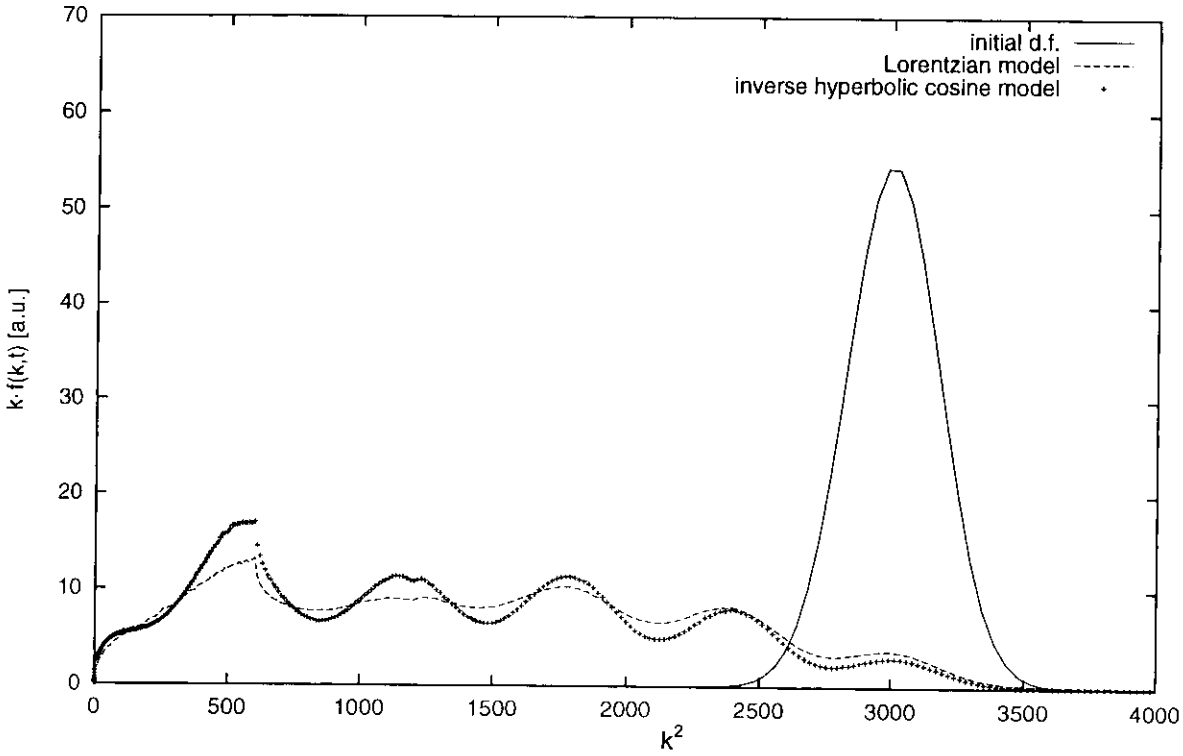

Fig. 4. Comparison of the electron distribution $k \cdot f(k,t)$ versus k^2 obtained by the two damping models for evolution time 600 fs. The particle transfer towards the subthreshold region is faster for the inverse hyperbolic cosine model

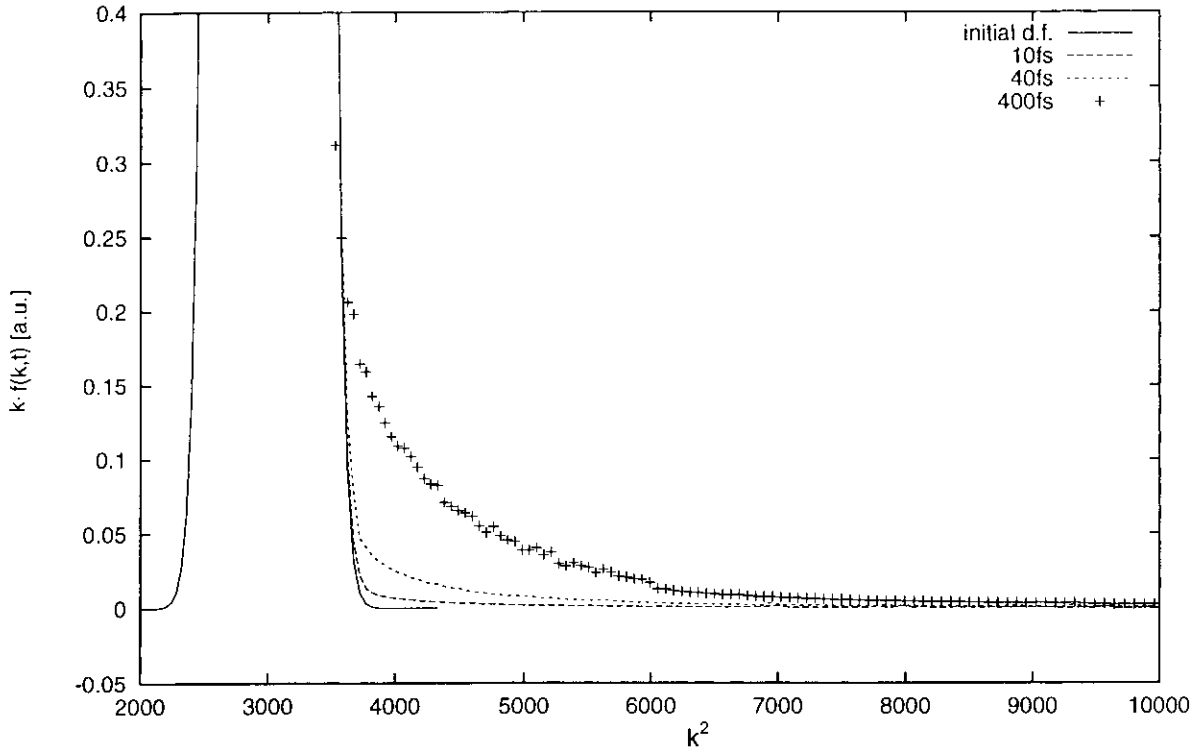

Fig. 5. The electron distribution $k \cdot f(k,t)$ versus k^2 in the region above the initial condition obtained by the Lorentzian model for evolution times 10, 40, and 400 fs. The run-away effect increases with the evolution time

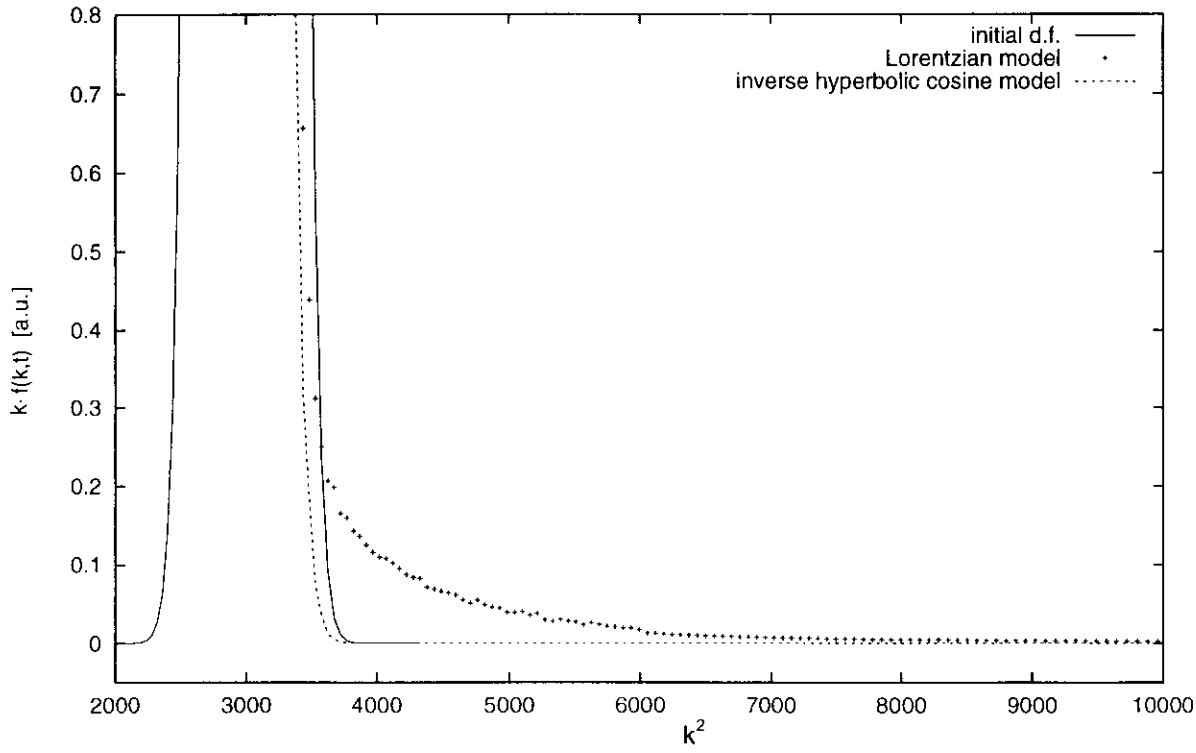

Fig. 6. Comparison of the electron distribution $k \cdot f(k,t)$ versus k^2 obtained by the two models for 400 fs evolution time. The run-away effect is not presented in the inverse hyperbolic cosine model

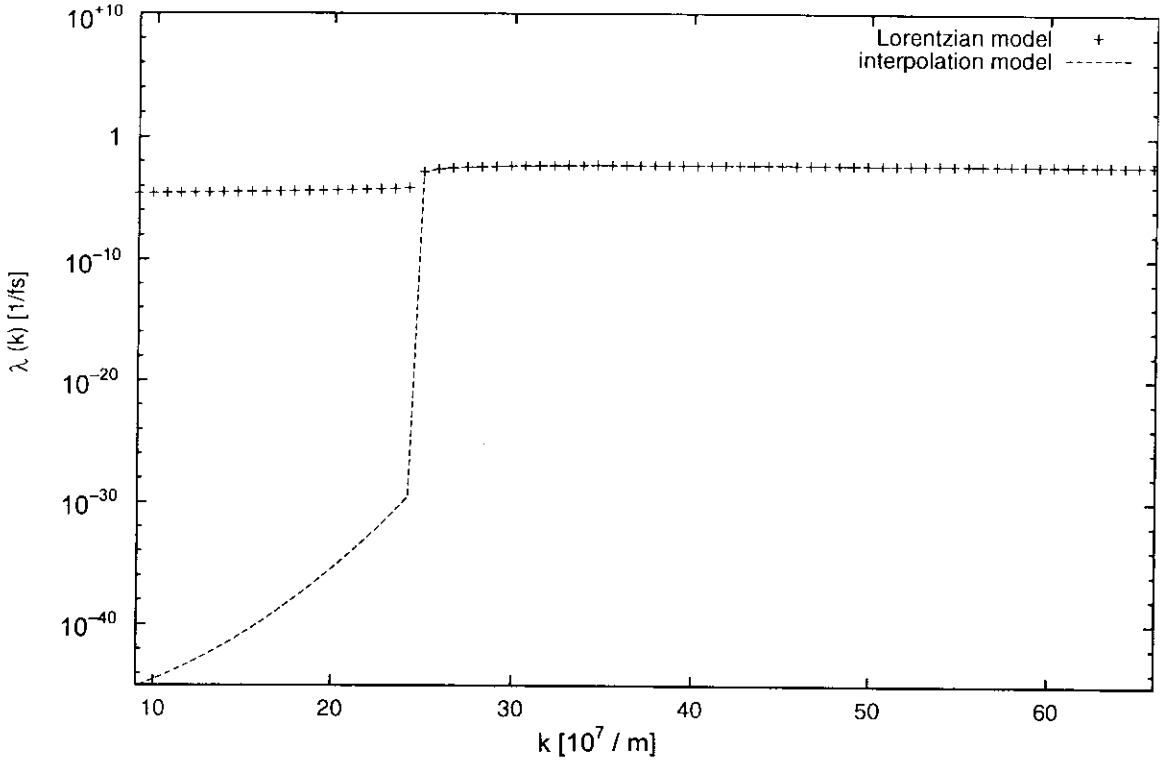

Fig. 7. Comparison of the total out-scattering rate $\lambda(k)$ in logarithmic scale versus k for the two models. λ and k are in units 1/fs and 10^7/m, respectively. The variation of λ above the threshold for the two models and below the threshold for the Lorentzian model is below one order of magnitude, so that, in this scale, their behaviour looks rather flat. Below the threshold, the out-scattering rate for the classical Boltzmann equation is exactly zero. In the inverse hyperbolic model an out-scattering event happens once per 10^{30} fs, i.e. is practically zero. The Lorentzian model out-scattering rate remains finite for the Boltzmann transport time scale

initial region. For longer times the run-away effect will just continue in form of further heating of the electron gas.

The inverse hyperbolic cosine model does not exhibit such an effect, as can be seen from the comparison of the 400 fs solutions of the corresponding models, Fig. 6.

Fig. 7. compares the total out-scattering rates of the two models. The Lorentzian gives a finite probability for the electron to be scattered out of the states below the phonon energy. This means that there are events, in which the electron can gain energy from the lattice which is supposed to have no energy. The effect is suppressed in the inverse hyperbolic cosine model, where λ is practically zero. Since the rates are time independent, the effects remain for any evolution time. Thus, for very long times the Lorentzian model gives rise to deviations from the equilibrium distribution, while the inverse hyperbolic cosine distribution function is close to the equilibrium one.

The Markovian limit of the one-band quantum kinetic model has major contribution to the intermediate-time-scale evolution and determines the solution for large times. It introduces phenomena such as the run-away effect and out-scattering processes under the phonon threshold. This indicates that the behaviour of the model carrier system contains unrealistic effects. The inverse hyperbolic cosine model does not introduce such effects in the carrier kinetics. It corrects properly the one-band model, thus providing an more adequate description of the evolution process.

A Monte Carlo approach for solving a Boltzmann-like transport equation with isotropic initial conditions has been developed. It simulates effectively one-dimensional equations, while in this case the common Ensemble Monte Carlo algorithm must be carried out in three dimensions. The approach provides a possibility to find the solution in a fixed phase space point, without being necessary to solve the equation in the whole definition domain. It should be noted, that the common numerical approaches, based on finite difference schemes cannot clearly reveal the considered discontinuity of the distribution function, since such schemes suppose a continuity of the solution f. The ICFE can be easily incorporated in the algorithm. The algorithm is inherently parallel. The approach allowed to study rather accurately the differences between different damping models.

Appendix

The resolvent terms $\mathcal{K}_i\phi$ of the solution of an integral equation

$$f(x) = \int \mathrm{d}x' \, \mathcal{K}(x, x') \, f(x') + \phi(x) \tag{9}$$

are given by the following multiple integrals:

$$(\mathcal{K}_i\phi)(x_0) = \int \ldots \int \mathcal{K}(x_0, x_1) \ldots \mathcal{K}(x_{i-1}, x_i) \, \phi(x_i) \, \mathrm{d}x_1 \ldots \mathrm{d}x_i \, .$$

The applied Monte Carlo method [10], is based on the following estimator:

$$v_i = \frac{\mathcal{K}(x_0, x_1)}{P(x_0, x_1)} \cdots \frac{\mathcal{K}(x_{i-1}, x_i)}{P(x_{i-1}, x_i)} \, \phi(x_i)$$

which is used further to provide the solution in the fixed point x_0. The transition probability density P can be arbitrary, but it should satisfy the requirement to be different from zero in the points where the kernel $\mathcal{K}$ is not zero, and should be normalized: $\int \mathrm{d}x' \, P(x, x') = 1 \quad \forall x$.

The method ensures a direct control of the numerical precision in the desired point. This allows to evaluate effects, e.g. the run-away effect, occuring two to four orders of magnitude below the peak of the initial distribution for a very reasonable simulation time.

A smart choice of the transition probability increases further the efficiency of the algorithm. Here we choose it to be proportional to a Lorentzian with a $\Gamma(k)$, replaced with a suitable constant. For any before-scattering state k the Lorentzian is divided by its integral on the after-scattering states k' because of the normalization. Then an analytic dependence of k' on k and the selected by the random generator value $\ni$ is possible. A numerical trajectory consisting of the points x_0 (fixed), $x_1, \ldots, x_i$ is then constructed N times. The mean value of the estimator with respect to these N independent realizations gives the contribution of the i-th iteration term to the solution. In the code for each numerical trajectory we calculate the estimator values corresponding to the two models. The output provides the two solutions with only one trajectory construction procedure, thus reducing the necessary simulation time.

References

[1] H. HAUG and S.W. KOCH, Quantum Theory of the Optical and Electronic Properties of Semiconductors, 3rd ed., World Scientific, Singapore 1994.
[2] J.SCHILP, T. KUHN, and G. MAHLER, Phys. Rev. B **50**, 8 (1994).

[3] I. LEVINSON, Soviet Phys. – JETP **30**, 362 (1970).
[4] J. RAMMER, Rev. Mod. Phys. **63**, 781 (1991).
[5] J. BARKER, J. Phys. C **6**, 2663 (1973).
[6] L. REGGIANI and P. LUGLI, Phys. Rev. B **36**, 6602 (1987).
[7] R. ZIMMERMANN, phys. stat. sol. (b) **159**, 317 (1990).
[8] D.B. TRAN THOAI and H. HAUG, Phys. Rev. B **47**, 3574 (1993).
[9] H. HAUG and L. BANYAI, Solid State Commun. **100**, 303 (1996).
[10] M. NEDJALKOV, T. GUROV, and I. DIMOV, Math. Comput. Simul., in print.
[11] T. KUHN and F. ROSSI, Phys. Rev. B **46**, 12 (1992).
[12] C. JACOBONI, P. POLI, and L. ROTA, Solid State Electronics **31**, 523 (1988).
[13] H. HAUG and A.P. JAUHO, Quantum Kinetics for Transport and Optics in Semiconductors, Springer-Verlag, Berlin 1996.
[14] L. BÁNYAI, H. HAUG, and P. GARTNER, Europ. Phys. J. B **1**, 209 (1998).